Nonlinear interaction of ring dark solitary waves with coaxial dark beams

A. Dreischuh[a], D. Neshev[a], S. Chervenkov[a], G. G. Paulus[b], F. Grasbon[b], H. Walther[b,c]

[a]Sofia University, Department of Quantum Electronics, 5, J. Bourchier Blvd., BG-1164 Sofia, Bulgaria

[b]Max-Planck-Institut für Quantenoptik, Hans-Kopfermann-Str. 1, D-85748 Garching, Germany

[c]Ludwig-Maximillians-Universität, Sektion Physik, Am Coulombwall 1, D-85747 Garching, Germany

ABSTRACT

Theoretical and experimental results on optical ring dark solitary waves are presented, emphasizing the interplay between initial dark beam contrast, phase-shift magnitude, background-beam intensity and saturation of the nonlinearity. An enhanced RDSW transverse dynamics originating in the interaction with a second coaxial dark beam is analyzed theoretically in a good agreement with the experiment. The results may open the way to construct a parallel all-optical three-position radial switch.

Keywords: phase dislocation, ring dark solitary wave, optical vortex, nonlinear interaction

1. INTRODUCTION

Mathematically, optical dark spatial solitons are exact solutions of the one-dimensional nonlinear Schrödinger equation (NLSE) for negative nonlinearity and nonvanishing boundary conditions. Physically, they form on background beams of finite width as self-supported intensity dips due to the counterbalance between beam self-defocusing and diffraction. Losses, saturation and high transverse dimensionality result in nonintegrable model equations. Despite certain adiabatic relaxation characteristics, the solitary solutions of these equations have a large number of characteristics[1] in common with the soliton solution of the one-dimensional NLSE and are widely denoted by the term "dark soliton". Optical ring dark solitary waves (RDSWs) were first introduced by Kivshar and Yang[2]. The quasi-one-dimensional treatment allowed the authors to obtain an expression for the RDSW's transverse velocity dR/dz as a function of the ring radius R(z=0) and the contrast. The first experimental generation of optical RDSWs[3] was conducted with pure amplitude modulation in front of the nonlinear medium. In a subsequent experiment[4] RDSWs were generated from odd initial conditions by using binary computer-generated holograms (CGHs). The RDSWs may turn out to be of practical interest because of their ability to induce waveguides in which multiple signal beams could be guided parallel[5]. The effective control of the RDSW transverse dynamics may open the way to construct a parallel all-optical radial switch. This idea inspired the present analysis.

2. INTRINSIC RDSW DYNAMICS

2.1. Model equation and parameter range

The numerical simulations carried out are based on the generalized NLSE

$$-i2k_0 n_0 \frac{\partial E}{\partial z} + \left(\frac{\partial}{\partial x^2} + \frac{\partial}{\partial y^2} \right) E + k_0^2 f\left(|E|^2\right) E = 0 \qquad (1)$$

which accounts for the two-dimensional beam diffraction and medium nonlinearity. The equation is solved by the beam propagation method over a 1024x1024grid. The saturation model $f(I) \sim I/(1+I/I_{sat})^3$ for the nonlinearity corresponds to the best sigmoidal fit of the experimental data extracted from a background-beam self-deflection experiment (Fig. 1, solid curve). The intensity I_{sol}^{1D} required for one-dimensional dark spatial soliton formation is used to estimate the saturation $s=I/I_{sat}$ of the nonlinearity in the experiment. Briefly, single-line Ar^+-laser (λ=488 nm) is used to reconstruct the respective CGH. The latter are produced photolithographically with a grating period of 18 μm and ensure a diffraction efficiency of nearly 10% in first order. The nonlinear medium (NLM) is ethylene glycol dyed with DODCI (Lambdachrome). The background beam diffracted in first order with the dark beam(s) nested in is transmitted through a slit and is gently focused on the entrance of the NLM. After passing the desired nonlinear propagation path length (0.5 cm to 8.5 cm) it is

11th International School on Quantum Electronics: Laser Physics and Applications, Peter A. Atanasov, Stefka Cartaleva, Editors, Proceedings of SPIE Vol. 4397 (2001) © 2001 SPIE · 0277-786X/01/$15.00

partially reflected by a prism immersed in the liquid and is projected directly on a co-moving CCD array with a resolution of 13 μm. The maximum NLM length or 10 cm is found to correspond to 4.4 nonlinear lengths L_{NL}, whereas the CGH-to-NLM distance is estimated to be approximately four Rayleigh diffraction lengths L_{diff}.

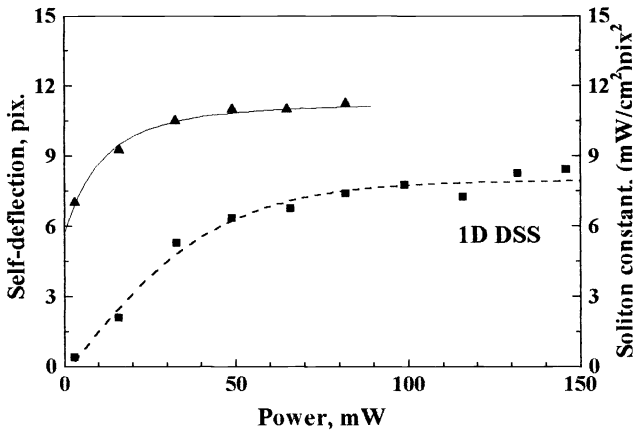

Fig. 1 Power dependencies of the background-beam self-deflection (triangles) and of the quantity $I_{sol}^{1D}=Ia^2$ (squares) indicating $P_{sat}\approx$35mW and $P_{sol}^{1D}\approx$90 mW.

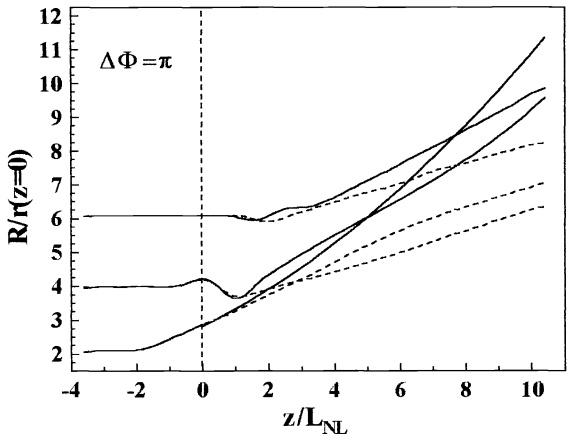

Fig. 2 Diffraction-governed evolution of RDSWs with initial π jumps over $4L_{diff}$ followed by nonlinear propagation in a Kerr (s=0, solid curves) and saturable Kerr-like medium (s=0.4, dashed curves). Vertical dashed line - the nonlinear interface.

Initially "black" RDSWs with high transverse dynamics are not likely to be present in a real experiment, at least when generated by holograms. The reason consists in the necessity to select one of the diffracted beams, that requires a certain free-space propagation. After some diffraction is "accumulated", the dark rings with small radii spread out substantially and their contrast decreases. Dark rings with large radii are less affected and evolve more slowly inside the NLM. Fig. 2 is intended to visualize this before and inside the NLM. Solid and dashed lines correspond to Kerr and saturable Kerr nonlinearity ($s=I/I_{sat}=0.4$). The simulation refer to $I=I_{sol}^{1D}$ and to an initial phase jump of π, which will be flattened in the course of propagation. Generally, the saturation of the nonlinearity leads to reduction of the RDSW dynamics.

2.2. Power dependence of the transverse velocity

In this experiment we observed a well-pronounced non-monotonic change of the ring radius vs. background beam power (Fig. 3a). Unfortunately it is not strong enough to allow to distinguish between three separate RDSW spatial positions and can not be used to construct a parallel all-optical radial switch. Nevertheless, from this dependence one can gain an insight in the intrinsic RDSW dynamics. In Fig. 3b we plot the corresponding data for the RDSW contrast $A^2=(I_0-I_{min})/I_0$. Generally, the reversed non-monotonic behaviour is consistent with the intuition that the smaller the ring, the higher the total phase shift, the darker the solitary wave, and the better the signal-beam guiding ability. The detailed numerical simulations showed that the non-monotonic power dependencies are due to the enhancement of the phase shift and the contrast of the RDSW by saturating the nonlinearity.

2. PHASE-DEPENDENCE OF THE TRANSVERSE VELOCITY

As mentioned, initially "black" RDSWs with high transverse dynamics are not likely to be present in an experiment, when they are generated by CGHs. The experimental data and the comparative numerical simulations showed that there is no difference whether the phase inside the ring Φ_{in} is bigger or lower than the phase Φ_{out} outside the ring, when $|\Phi_{in}-\Phi_{out}|=\pi$. Equivalently, there should be no difference in the transverse dynamics of the RDSWs generated by the +1-st and -1-st diffraction order beam when a π phase jump is encoded in the CGHs. The situation changes when the magnitude of the initial phase jump is less than π (see Fig. 4). Numerical simulations are carried out by keeping the following parameters close to the experimental values: initial dark ring radius-to-width ratio $(R/r)|_{z=0}=2$, 4, and 6, background beam intensity $I=I_{sol}^{1D}$, initial contrast $A^2==0.88$, phase jump $\Delta\Phi|_{z=0}=0.837\pi$, and saturation of the nonlinearity s=0.4. In Fig. 4a we show

results corresponding to the case of a higher phase inside the rings $\Phi_{in}>\Phi_{out}$. The effective convex wavefront inside the RDSW forces the ring to broaden faster as compared to the case of an initial π phase jump. The data plotted in Fig. 4b refer to the case of a lower phase inside the dark ring and higher phase outside ($\Phi_{in}<\Phi_{out}$). The effective concave wavefront forces the RDSWs to collapse to a minimum ring diameter. Thereafter they start to broaden faster. The main tendency, that the

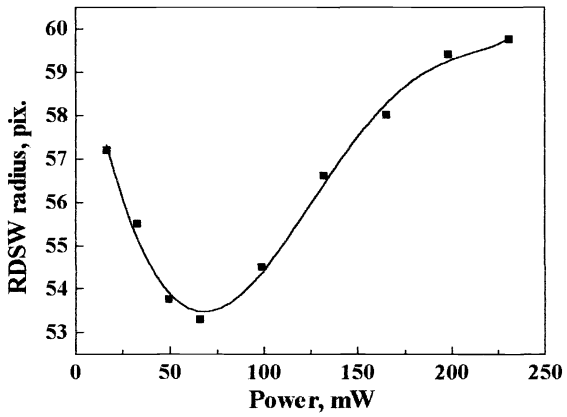

Fig. 3a Power dependence of the RDSW radius after nonlinear propagation path length z=8.5 cm.

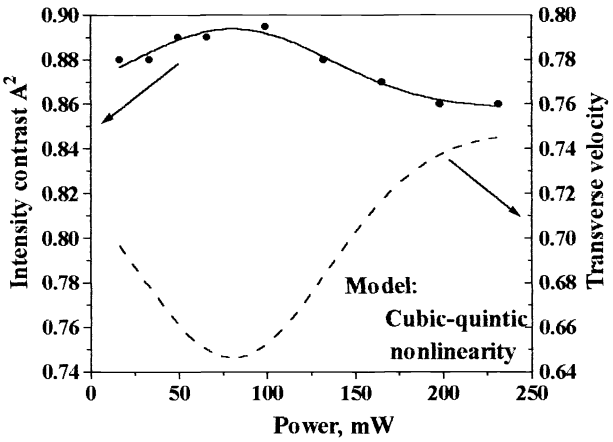

Fig. 3b Power dependence of the RDSW contrast (dots) and estimated transverse velocity (dashed curve) for s=0.4.

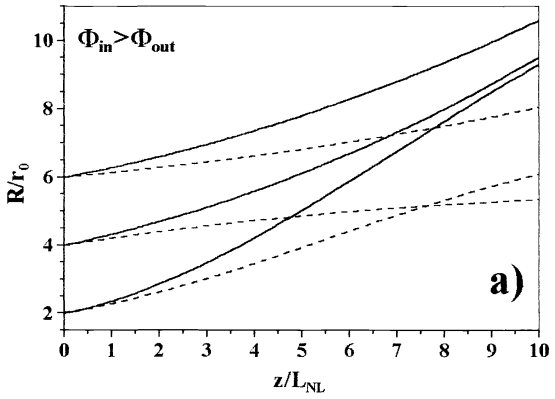

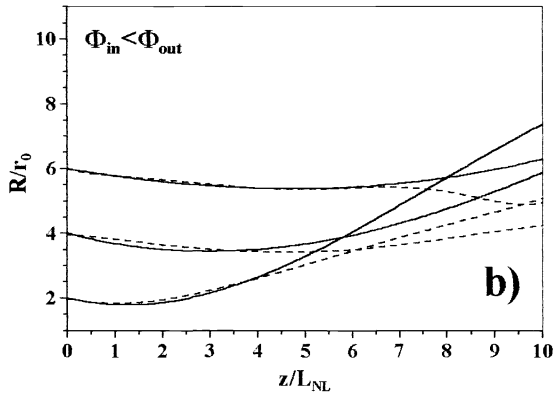

Fig. 4 Nonlinear evolution of initially grey RDSWs in a Kerr (solid curves) and saturable Kerr-like medium (dashed; s=0.4) for positive **(a)** and negative **(b)** phase shift $\Delta\Phi=\Phi_{in}-\Phi_{out}$. See text for details.

broader the RDSW initially is, the longer nonlinear propagation is needed to reach R_{min}, is well expressed. The other general tendency, that the smaller the RDSW diameter is, the higher its transverse dynamics is, can also be clearly seen.

3. NONLINEAR INTERACTION WITH COAXIAL DARK BEAMS

The nonlinear interaction of a RDSW with a second coaxial dark beam provides the most effective way to control the dark ring transverse dynamics. The frames shown in Fig. 5 are recorded by imaging the used holograms directly on the CCD-array. Generally, the interaction potential between opposite phase dislocations is repulsive. Coaxial optical vortex (OV) should increase the transverse velocity of the RDSW (Fig. 5, left frame), whereas a second outlying RDSW should decrease it (Fig. 5, right frame). This repulsion is evident from the diffraction-governed evolution of the dark ring radius (Fig. 6). In our numerical simulations we modeled the free-space propagation of a RDSW over $4L_{diff}$ followed by nonlinear propagation in a saturable Kerr-like medium (Fig. 7). The middle curve (1) refers to a single RDSW generated from a CGH with an encoded π phase jump. Because of the relatively large dark ring radius-to-width ratio R/r =4 at z/L_{Diff}=-4, the ring diameter remains nearly unchanged at the entrance of the NLM. The linear interaction with a second coaxial dark beam does not affect significantly the dark ring radius provided it is generated with an initial π phase jump (Fig. 7, both

dashed curves). The gradually higher dark ring transverse dynamics presented by the most upper and lower curves is due to the suitable choice of the grey initial conditions ($\Phi_{in} \neq \Phi_{out}$) of the ring generation. Let us concentrate further on the evolution inside the NLM. The effective convex phase front inside the ring for $\Phi_{in} > \Phi_{out}$ (see Fig. 4a) leads to an enhanced repulsion between the ring and the OV beam and the RDSW transverse velocity is high. In the opposite case, the effective convex phase front inside the ring for $\Phi_{in} < \Phi_{out}$ (see Fig. 4b) and the repulsion from the outer ring forces the RDSW to collapse near $z=(3.5\text{-}4)L_{NL}$. This collapse is followed by an approximate recovering of the initial ring radius at $z=10L_{NL}$. According to the adopted style of designation of the curves, 1 means a single RDSW generated with an initial π phase jump, 2 - two coaxial RDSWs (the outer one with an initial π phase jump, the inner - with $\Phi_{in} < \Phi_{out}$) , whereas 1+1 refers to an initially grey RDSW (with $\Phi_{in} > \Phi_{out}$) and a coaxial OV beam. The grey RDSWs were encoded in the respective holograms with magnitude of the phase jump $\Delta\Phi = 2\pi/3$.

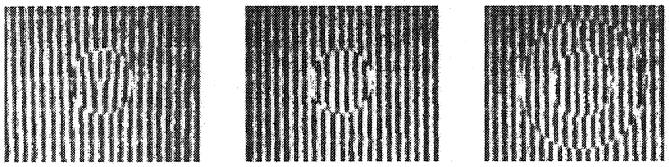

Fig. 5 Structure of the CGHs for generating a single RDSW (middle), RDSW and a coaxial optical vortex beam (left), and two coaxial RDSWs (right).

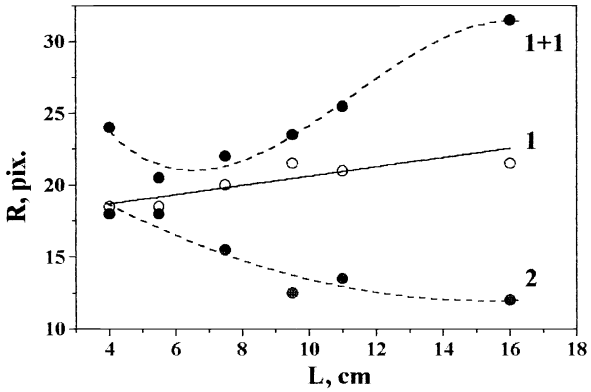

Fig. 6 Diffraction-governed evolution of the dark ring (1 and 2 - single and two coaxial dark rings, respectively, 1+1 - dark ring with an optical vortex nested in).

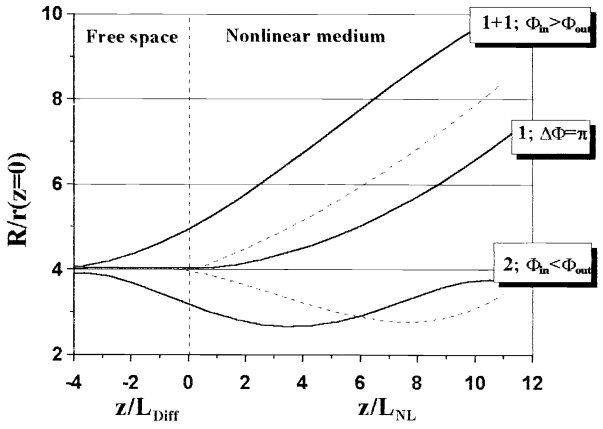

Fig. 7 Numerical simulations: Diffraction-governed evolution of RDSW with (1+1, 2) and without (1) second coaxial dark beam over $4L_{diff}$ followed by nonlinear propagation in a saturable Kerr-like medium (s=0.4). Vertical dashed line - the nonlinear interface. Most upper and lower solid curves - nonlinear interaction with an OV beam and a second RDSW when the RDSW is generated as a grey one. Dashed curves- nonlinear interaction when the RDSW is generated with an initial π phase jump.

We measured experimentally the evolution or the RDSW radius along the thermal NLM up to z=2.5 cm. The absorption at λ=488 nm was estimated to be α=0.2 cm^{-1}, which corresponds to a saturation coefficient s=0.75 for background beam power $P=1.2P_{sol}^{1D}$=30 mW. We observed asymptotically constant RDSW radii for propagation distances z>1.5 cm which result from both absorption and NLM saturation. In Fig. 8a we plot radial cross-sections of the recorded RDSWs after a nonlinear propagation of z=0.7 cm. The background-beam power is 30 mW, i.e. $P=1.2P_{sol}^{1D}$ and s=0.75. The vertical dashed lines are intended to visualize the imaginary radial "channels". The most inner "channel" C3 is formed by a RDSW which radial collapse is enhanced by the interaction with an outlying RDSW. The most outer "channel" C1 is gradually stronger deflected radially by the central OV beam. The middle "channel" C2 is supported by the single, initially "black" RDSW with a relatively low transverse dynamics. Fig. 9b is intended to visualize the imaginary "channel" disposition. For this purpose diametrical slices of the respective recorded frames are combined.

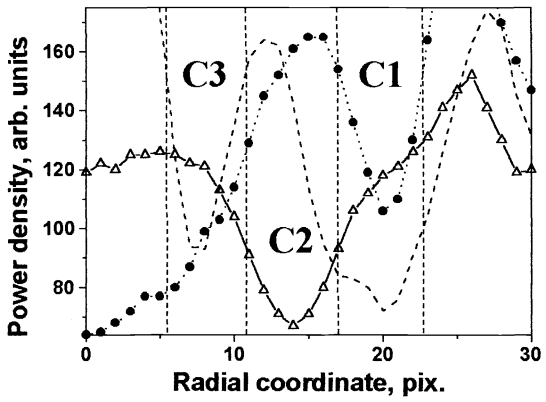

Fig. 8a Radial cross-section of the dark beams with the imaginary radial channels (C1-C3).

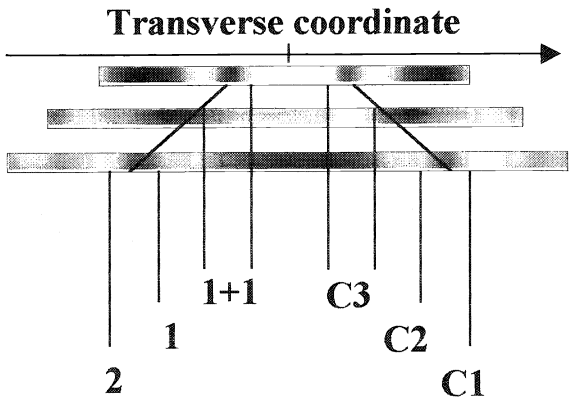

Fig. 8b Diametrical greyscale-coded slices of the dark beams. The type of the interacting waves and the imaginary radial channels are denoted according the adopted convention (see text).

5. CONCLUSION

The comparison between the corresponding curves in Fig. 4a,b and Fig. 7 clearly show that the suitable choice of the initial phase profile of the RDSW combined with the repulsive interaction with a second coaxial dark beam can lead to the generation of RDSWs with gradually enhanced transverse dynamics. On this base it may appear feasible to construct an all-optical radial switch for parallel signal beams/pulses. Further analyses are under way to estimate the guiding and switching efficiencies and to minimize the channel-to-channel cross-talk. Fast reconfiguration of such a radial switch can be done by using properly designed multiple-active electrically-controllable CGH.

ACKNOWLEDGMENTS

This work was supported by the Science Foundation of the Sofia University (Sofia, Bulgaria) and by the National Science Fund (Bulgaria). A.D. would like to thank the Alexander von Humboldt Foundation for the award of a fellowship.

REFERENCES

1. Yu. S. Kivshar, B. Luther-Davies, "Dark optical solitons: Physics and applications," *Physics Reports* **289**, pp. 81-197, 1998.
2. Yu. S. Kivshar, X. Yang, "Ring dark solitons, "*Phys. Rev.* **E50**, pp. R40-R43, 1994.
3. S. Balushev, A. Dreischuh, I. Velchev, S. Dinev, and O. Marazov, "Odd and even 2D dark spatial solitons," *Appl. Phys.* **B61**, pp. 121-124, 1995; ibid., "Generation and evolution of 2D dark spatial solitons," *Phys. Rev.* **E52**, pp. 5517-5523, 1995.
4. D. Neshev, A. Dreischuh, V. Kamenov, I. Stefanov, S. Dinev, W. Fliepβer, and L. Windholz, "Generation and intrinsic dynamics of ring dark solitary waves," *Appl. Phys.* **B64**, pp. 429-433, 1997.
5. A. Dreischuh, V. Kamenov, and S. Dinev, "Parallel guiding of signal beams by a ring dark soliton," *Appl. Phys.* **B63**, pp. 145-150, 1996.